Bioorganic & Medicinal Chemistry Letters 23 (2013) 6141–6145

Contents lists available at ScienceDirect

Bioorganic & Medicinal Chemistry Letters

journal homepage: www.elsevier.com/locate/bmcl

Discovery of a potent, selective, and orally bioavailable histamine H_3 receptor antagonist SAR110068 for the treatment of sleep–wake disorders

Zhongli Gao [a,*], William J. Hurst [b,†], Werngard Czechtizky [d], Dominique Francon [c], Guy Griebel [c], Raisa Nagorny [b], Philippe Pichat [c], Lothar Schwink [d], Siegfried Stengelin [d], James A. Hendrix [b,‡], Pascal G. George [c]

[a] LGCR SMRPD Chemical Research, Sanofi US, 153-1-122, 153 2nd Ave, Waltham, MA 02451, USA
[b] Sanofi US, 55C-420A, 55 Corporate Drive, Bridgewater, NJ 08807, USA
[c] Sanofi R&D, Chilly-Mazarin, France
[d] Sanofi R&D, Sanofi-Aventis Deutschland GmbH, Industriepark Hoechst, 65926 Frankfurt, Germany

ARTICLE INFO

Article history:
Received 29 July 2013
Revised 30 August 2013
Accepted 3 September 2013
Available online 8 September 2013

Keywords:
Histamine H_3 receptor antagonist/inverse agonist
GPCR
Awakening
EEG
Neurotransmitters (acetylcholine, noradrenaline, dopamine, GABA and serotonin)

ABSTRACT

Previous studies have shown that compound **1** displayed high affinity towards histamine H_3 receptor (H_3R), (human (h-H_3R), K_i = 8.6 nM, rhesus monkey (rh-H_3R), K_i = 1.2 nM, and rat (r-H_3R), K_i = 16.5 nM), but exhibited high affinity for hERG channel. Herein, we report the discovery of a novel, potent, and highly selective H_3R antagonist/inverse agonist **5a**(***SS***) (SAR110068) with acceptable hERG channel selectivity and desirable pharmacological and pharmacokinetic properties through lead optimization sequence. The significant awakening effects of **5a**(***SS***) on sleep–wake cycles studied by using EEG recording in rats during their light phase support its potential therapeutic utility in human sleep–wake disorders.

The histamine H_3 receptor (H_3R),[1] a $G\alpha_{I/O}$-protein coupled receptor, is a presynaptic autoreceptor damping the firing frequency of histamine neurons and inhibiting the histamine synthesis and release from axonal varicosities. H_3R has also been demonstrated to be heteroreceptors on axons of the most other neuro-transmitters (acetylcholine, norepinephrine, dopamine, GABA and serotonin), allowing powerful control over multiple homeostatic functions. Histaminergic neurons are located exclusively in the posterior hypothalamus from where they project to most areas of the central nervous system. Preclinically, H_3R antagonists/inverse agonists have demonstrated efficacies in a number of CNS pathologies including Alzheimer's disease,[2,3] attention deficit hyperactivity disorder,[4,5] schizophrenia,[6] sleep disorder,[7] neuropathic pain,[8] and obesity.[9] Several clinical candidates to address these diseases have been disclosed (for review articles, see Refs. [10,11]).

Narcolepsy is a rare disabling sleep disorder characterized by excessive daytime sleepiness (EDS) and abnormal rapid eye movement (REM) sleep manifestations including cataplexy (sudden loss of muscle tone). It has been reported that adult patients with narcolepsy exhibit decreased secretion of histamine in the cerebrospinal fluid. The blockade of histamine H_3 autoreceptor by Pitolisant (BF2-649),[4] a H_3R antagonist/inverse agonist, increased brain histamine and alertness in animal models of narcolepsy and improved alertness in adults with narcolepsy in an open pilot study.[7] However, no drug has been approved for this condition to date. There is an unmet medical need for a safe and efficacious treatment devoid of psycho-stimulate activities associated with drugs like amphetamine and modafinil, prompted us to embark on the discovery and development of a novel, potent, and highly selective H_3R antagonist/inverse agonist for treatment of sleep–wake disorders such as narcolepsy.

* Corresponding author. Tel.: +1 781 434 3635.
E-mail addresses: zhongli.gao@sanofi.com (Z. Gao), william.hurst@sanofi.com (W.J. Hurst), jhendrix@oligomerix.com (J.A. Hendrix).
† Tel.: +1 908 981 3723.
‡ Currently at: Oligomerix Inc., 3960 Broadway, Suite 340D, New York, NY 10032, USA. Tel.: +1 212 568 0365.

0960-894X/$ - see front matter © 2013 Elsevier Ltd. All rights reserved.
http://dx.doi.org/10.1016/j.bmcl.2013.09.006

Previous work[12,13] from our group described a series of H_3R antagonists/inverse agonists, represented by 5-fluoro-2-methyl-*N*-[2-methyl-4-(2-methyl-[1, 3′]bipyrrolidinyl-1′-yl) phenyl] benzamide (**1**), that displayed oral efficacy in a mouse food intake inhibition model. In our on-going program aimed at the discovery of a 'best in class' H_3R antagonist/inverse agonist, that is potent with lower species discrepancy; high selectivity towards a panel of GPCRs, ion channels, enzymes and kinases, particularly biogenic amine receptors; desirable PK profile suitable for *qd* dosing in human; and acceptable neuropsychological, behavioral, and cardiovascular safety in experimental animal models; and superior hERG channel selectivity. Besides these specific requirements, we set up an additional criterion of a lower risk of potential phospholipidosis induction, one of the common issues of H_3R antagonists/inverse agonists reported in the literature.[14,15] Herein, we describe the optimization sequence leading to **5a**(***SS***) (SAR110068).

We took the multipronged strategy in which the H_3R affinities and calculated physico-chemical properties, such as molecular weight, number of hydrogen bond donors and acceptors, number of rotatable bonds, *c*log*P*, and polar surface area (calculated using ACD/Labs methods) were considered in a ballanced manner. The present work was the continuation of optimization effort from the previous series to only solve the hERG channel selectivity issue. The plan was not to modify the Me-pyrrolidine or its vicinity but only the amide moiety. Therefore, the pK_a, polar surface area, and molecule weight were slightly different or the same among the ligands we discussed herein. As said, the optimization was mainly driven by H_3R affinity and *c*log*P*.

From previous SAR, it was evident that the left side aromatic ring with small lipophilic substituents was required for good H_3R affinity. Unfortunately, lipophilic substituents in the aromatic ring also adversely increased hERG channel affinity and phospholipidosis liability. Levoin et al.[16] reported a QSAR approach in which the authors concluded that lipophilic character of the molecules (the sum of atomic polarizabilities, *c*log*P*, *c*log*D*), as well as aromatic tendency had the greatest influence over hERG affinity.

Phospholipidosis is a storage disorder resulting in excessive accumulation of phospholipids in lysosomes of the tissues. The cause is not well defined. However, the amphiphilic type of molecules display high risk for induction of phospholipidosis. In order to increase our odds to identify an ideal molecule with the lowest risk of phospholipidosis induction potential, we chose to use the in silico phospholipidosis model.[17,18] Given the fact that H_3R is a biogenic amine receptor and our current lead compound possessed a basic amine, it was hypothesized that increasing the polarity (lowering *c*log*P*), and reduce the aromaticity, should be the most direct approach to bring the calculated values into a more desirable range. To this end, it was envisioned that replacing substituted aryl moiety with cyclic-non-aromatic residues in the terminal end of the amide (Fig. 1) would achieve the objective mentioned above. Consequently, a new series of cyclic-non-aromatic amide **2** was designed.

The syntheses of the analogs **2a**–**2n** are described in Scheme 1. Aniline **3** (R^1 = H, 2′-CH_3, 2′-CF_3, and 3′-CH_3)[12,13] was coupled with proper acids or acid chlorides to obtain the desired compounds in high yield (75–82%).

Reagents and conditions: (a) RCOCl, CH_2Cl_2, pyridine, rt, 16 h, 62–88% yield; or RCO_2H, CH_2Cl_2, DMF, EDC·HCl, HOBt, *N*-methylmorpholine, rt, overnight, 75–82% yield.

Compounds (**2a**–**2n**) were then evaluated in an H_3R binding assay[13] by displacement of [^{3}H]*N*-α-methylhistamine in membranes isolated from a CHO cell line stably transfected with the rhesus monkey H_3 receptors (rh-H_3R) (Table 1).

The first compound synthesized and tested was **2a**, a cyclohexanecarboxylic amide instead of substituted phenyl carboxylic amide, to ensure similar relative size of the ligand's terminal moiety. The compound was active with a K_i of 9.0 nM. Encouraged by this data, we decided to explore further on cyclic-non-aromatic carboxamides. A decrease of structural flexibility by introducing a bridge in the cyclohexyl ring (**2c**) did not enhance the affinity. Instead, the affinity decreased by twofold compared to **2a**, indicating that steric bulkness was not well tolerated in this region of the ligand. This observation was echoed by the fact that compound **2f** was equipotent to **2a**, while **2j** displayed a fourfold decrease in affinity. However, extension of the cycloalkyl by a methylene linker is tolerated as exemplified by **2m**. Another trend of the SAR was that the analogs of R^1 = 2′-Me were more potent than analogs of R^1 = 3′-Me (**2c** vs **2d**; **2f** vs **2h**; **2j** vs **2k**; **2m** vs **2n**), while the analogs of R^1 = H were comparable in H_3R affinity with that of R^1 = 2′-Me. This trend was consistent with the previous SAR studied with the aryl amide series in which the 2′-methyl was important in enhancing activity at H_3R and also improving the metabolic stability. The enhancing effect of the 2′-Me might attribute to its ability of maintaining the preferred confirmation of the ligand to better fit the contour of the H_3R receptor as hypothesized previously.[12]

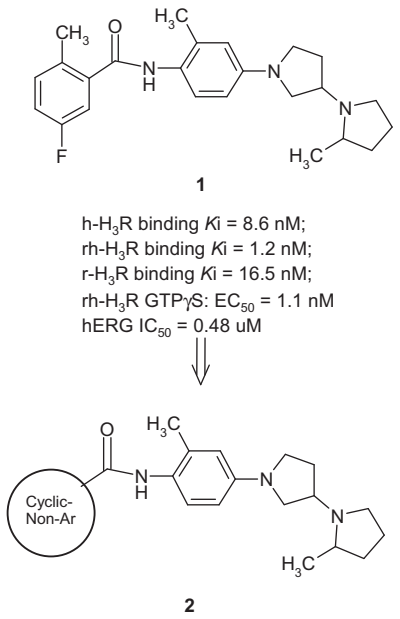

Figure 1. Structure of the lead **1** and the optimization strategy.

The *c*log*P* (data see Table 1) was not in the desired range of 1.5–2.5 for CNS penetration for most of the compounds in Table 1. Further optimization was necessary.

In order to decrease *c*log*P* while maintain H_3R affinity for this series of the compounds, the strategy would be to make the smallest structural modification possible. To achieve this objective, introduction of heteroatoms into the left side cycloalkyl moiety was proposed. Thus, compound **4a** (Table 2) was synthesized and tested. The affinity was, fortunately, comparable with the cyclic carboxamide **2a**. The analog **4d** was comparable with **4a** in H_3R affinity, while **4g** was an eightfold less potent than **4a** (Table 2). Similarly, the analogs of R^1 = 2′-Me were more potent than analogs of R^1 = 3′-Me (**4a** vs **4b**; **4d** vs **4e**). However, **4g** was comparable with **4h** in this case; while the analogs of R^1 = H were comparable with that of R^1 = 2′-Me (**4c** vs **4d**).

We then turned our attention towards the stereochemistry effect on H_3R affinity in this series. In this endeavor, we narrowed down to the analogs where R1 = 2′-Me because of its superior H_3R affinity and metabolic benefits as mentioned above. Thus two stereoisomers, **5a**(***SS***) and **5a**(***RS***), corresponding to the more

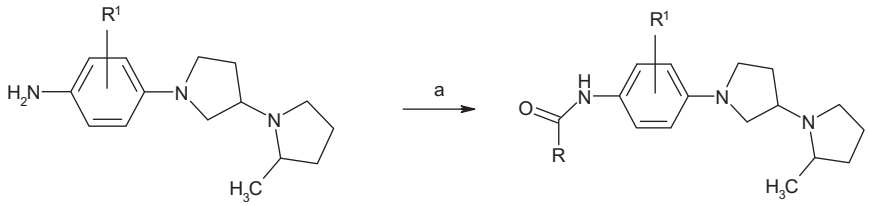

3 2

Scheme 1. Syntheses of analogs **2a**–**2n**.

Table 1

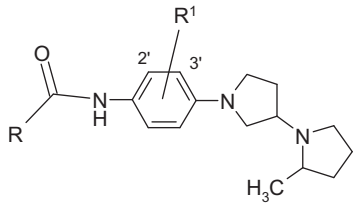

2

No.	R	R^1	rh-H_3R binding K_i[a] (nM)	*c*log*P*
1	2-Me, 5-F-Ph-	2′-Me	8.6	4.4
2a	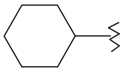	2′-Me	9.0	3.8
2b	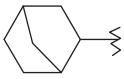	H	15.7	3.9
2c		2′-Me	19.9	3.9
2d		3′-Me	130.3	4.4
2e	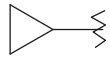	H	9.7	2.3
2f		2′-Me	9.6	2.3
2g		2′-CF3	14.7	2.4
2h		3′-Me	17.7	2.7
2i	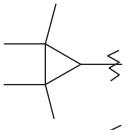	H	143.8	4.1
2j		2′-Me	37.3	4.1
2k		3′-Me	65.5	4.6
2l	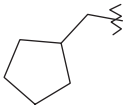	H	3.1	3.9
2m		2′-Me	8.4	3.8
2n		3′-Me	10.7	4.3

[a] K_i values were an average of three or more determinations.

potent amide **4a** was synthesized and tested (Table 3). The 2*S*, 3*S* stereoisomer, **5a** (***SS***),[19] demonstrated superior H_3R affinity over **5a** (***RS***). These results are consistent with the previous studies with the aryl carboxamide **1**.[19] The SAR for the wider range of amides was similarly explored with *2S*,*3S* stereoisomers. The H_3R affinity were uniformly high when compared with their corresponding diastereomeric mixture **2a**–**2n**, **4a**–**4h**, confirming that the *2S*,*3S* stereoisomer was the right choice. When examining *c*log*P*, **5a** and **5g** excelled while **5a**(***SS***) exhibited higher H_3R affinity. Consequently, **5a**(***SS***) was selected for further profiling.

Compound **5a**(***SS***)[20] was a crystalline material and showed a single polymorph when recrystallized from DCM and *t*-butyl methyl ether. Chiral HPLC gave 99.9% ee with $[\alpha]_D$ = + 29.35 (*c* 0.46, MeOH). Log*P* and log$D_{7.4}$ were determined to be 1.31 and 0.15, respectively. The compound was soluble in water (solubility = 1.1 mg/mL) and in a GI tract simulation medium (solubility >2.5 mg/mL). The compounds was stable in all solutions tested (water, aqueous solution of pH 1.0–7.4, DMSO, GI tract simulation medium) (<2% degradation over 48 h at rt).

In in vitro pharmacology, **5a**(***SS***) exhibited human H_3R affinity with K_i of 1.0 nM determined by displacement of [^{3}H]*N*-α-methylhistamine in membranes isolated from a CHO cell line stably transfected with human H_3 receptors (h-H_3R). In human H_3 (H445) CHO-CRE-Luc assay,[21] EC_{50} was determined to be 0.9 nM. Its functional behavior was confirmed as a competitive H_3R antagonist in a RAMH-induced inhibition of electrical field stimulated guinea pig ileum contractions model. The compound was also highly selective as indicated by CEREP in which its percent inhibition of control specific binding was <50% for 78 receptors and 16 enzymes (except σ 1 and/or 2 with 53% inhibition @ 10 μM) and 26 kinases and 38 ion channels.

Compound **5a**(***SS***) was also stable in the plasmas of human, guinea pig, rat, mouse, dog, monkey, sheep and rabbit. The percentage of biotransformation for **5a**(***SS***) in human microsomes in vitro was <5% with little or no metabolic liability in mouse, rat, guinea pig, rabbit, macaque and dog microsomes. In human hepatocytes in vitro, **5a**(***SS***) exhibited a low metabolic clearance at 0.031 ± 0.002 mL h^{-1} (106 hep)$^{-1}$ (n = 4) with low inter-preparation variability. At lower concentration (0.5 μM), the Cl_{int} did not increase indicating no concentration dependency of the in vitro metabolic clearance over this concentration range. CYP3A4 appeared to contribute to the overall metabolic clearance of this compound, with a contribution of 61 and 49% at 5 and 0.5 μM, respectively. CYP1A2, CYP2C9 and 2D6 seemed to be only slightly involved in **5a**(***SS***) metabolic clearance. In the in vivo pharmacokinetic studies, **5a**(***SS***) displayed low clearance (the *i.v.* Cl of 1.8 and 1.0 ng h/mL for mice and rats, respectively) and elimination half-life ($t_{1/2}$ = 2.3 h for mice; $t_{1/2}$ = 3.0 h for rat) with high exposure (AUC = 3.2 μg h/mL for mice, 8.4 μg h/mL for rat, both dosing at 10 mg/kg, *p.o.*) and acceptable oral bioavailability (58% in mice, 80% in rat) (Table 4). The brain AUC in mice and rats were 1.2 and 4.2 μg h/mL, respectively, when dosed orally at 10 mg/kg. The corresponding brain to plasma ratio was 0.35 and 0.33 for mice

Table 2

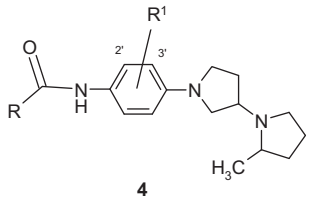

4

No.	R	R^1	rh-H_3R binding K_i[a] (nM)	*c*log*P*
4a	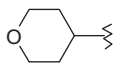	2′-Me	6.8	2.1
4b		3′-Me	17.0	2.6
4c	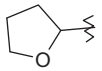	H	8.7	2.1
4d		2′-Me	7.34	1.9
4e		3′-Me	17.0	2.6
4f	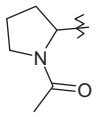	H	14.1	2.0
4g		2′-Me	57.7	2.0
4h		3′-Me	44.9	2.4

[a] K_i values were an average of three or more determinations.

Table 3

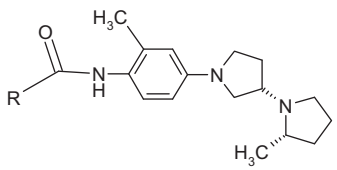

5(SS)

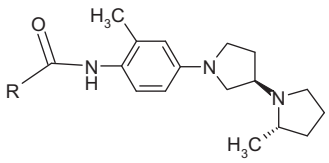

5(RS)

No.	R	rh-H_3R binding K_i[a] (nM)	*c*log*P*
5a(***SS***) (SAR110068)	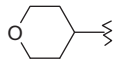	0.97	2.1
5a(***RS***)		3.90	2.1
5b(***SS***)	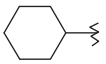	0.39	3.8
5c(***SS***)	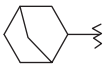	0.55	3.9
5d(***SS***)	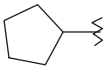	0.50	3.3
5e(***SS***)	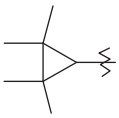	0.55	3.9
5f(***SS***)	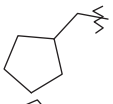	0.85	3.8
5g(***SS***)	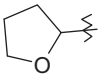	7.33	1.9

[a] K_i values were an average of three or more determinations.

Table 4

		Male OF1 Mice[a]		Male Sprague–Dawley rats[b]	
		Plasma	Brain	Plasma	Brain
i.v.	$AUC_{0\text{-inf}}$(ng h/mL)	1100	380	2100	700
	$t_{1/2}$ (h)	3.6	0.83	4.3	3.6
	Cl (ng h/mL)	1.8		1.0	
	Vd (L/kg)	3.5		3.1	
p.o.	AUC (ng h/mL)	3200	1200	8400	4200
	C_{max}	1870	765	1540	703
	t_{max}	0.17	0.50	1.0	1.0
	$t_{1/2}$ (h)	2.3	1.9	3.0	3.8
	F (%)	58		80	
	B/*P* ratio[c]		0.35		0.33

[a] Administration at 2 mg/kg *i.v.* and 10 mg/kg *p.o.*; *i.v.* formulation: 50% 1-methyl-2-pyrrolidinone in saline; concentration = 1.0 mg/mL, dosing 2 mL; *p.o.* formulation: 5% DMSO/0.5% MC/0.2%Tween80, concentration = 1.0 mg/mL; dosing 10.0 mL.

[b] Administration at 2 mg/kg *i.v.* and 10 mg/kg *p.o.*; *i.v.* formulation: Saline, concentration = 0.5 mg/mL; dosing 3.0 mL; *p.o.* formulation: 0.5% MC/0.2%Tween80; concentration = 1.0 mg/mL, dosing 10 mL.

[c] *B*/*P* ratio is brain to plasma ratio calculated with *i.v.* $AUC_{0\text{-inf}}$ exposure.

and rats, respectively, suggesting less concern for brain retention of the drug. Compound **5a**(***SS***) was well absorbed and CNS penetrable in rats and mice.

In in vitro drug safety assessment, **5a**(***SS***) did not induce any of the Cyp isoforms in human hepatocytes ($n = 4$; 1–60 μM), nor inhibit any of the Cyp isoforms (>100 μM), nor a substrate, nor an inhibitor of PGP, indicating low potential for the drug–drug interactions. The effect of **5a**(***SS***) on hERG current was investigated in vitro using patch-clamp technique in the whole-cell configuration on Chinese hamster ovary (CHO) cells stably transfected with the human gene of ERG. Compound **5a**(***SS***) inhibited hERG current with an IC_{50} = 18.9 μM ($n = 4$). The compound was negative in both Ames II assays (3–1000 μg/mL) and MNT (5–950 μg/mL) in the presence and in the absence of metabolic activation by human liver microsome preparations. Compound **5a**(***SS***) also showed a low risk of phospholipidosis induction potential in our internal in silico screen.[22]

In group toxicity studies (acute oral behavioral safety evaluation in mice), **5a**(***SS***) at oral dose of 30 mg/kg was well tolerated and showed no evidence of any behavioral side effects (social interaction, motility, preconvulsant and convulsions). Tremors were observed at 100 mg/kg, *p.o.*, only. This result was confirmed in an independent oral exploratory general behavior study (Irwin test) in male mice. There were no behavioral, neurologic, and autonomic effects observed when administrated orally at 0, 10, 30 mg/kg.

In cardiovascular safety evaluation, **5a**(***SS***) was assessed in anaesthetized cynomolgus monkeys. Administration of 10 mg/kg, *i.v.*, **5a**(***SS***) induced neither haemodynamic (blood arterial pressure and heart rate) nor electrocardiographic (PR, QRS, QTc intervals) effects. At this dose, plasma concentrations of **5a**(***SS***) measured at 5, 15 and 30 min post-dosing were 28, 14 and 11 μM, respectively.

Finally, the awakening effects of compound **5a**(***SS***) (SAR110068) were evaluated by using EEG [23] recording in rats during their light phase. Results showed that **5a**(***SS***) (3 and 10 mg/kg, *p.o.*) and thioperamide (10 mg/kg, *i.p.*) increased wakefulness and decreased slow wave and REM sleep to a similar degree than ciproxifan (10 mg/kg, *i.p.*), ABT0239 (10 mg/kg, *p.o.*) and GSK189254 (10 mg/kg, *p.o.*). Time-course analysis revealed that the awakening effects of thioperamide and GSK189254 lasted for about 1 h, while ciproxifan and ABT0239 produced such effects for 3 h. **5a**(***SS***) displayed the longest duration of awakening effects among the H_3R antagonists tested in our studies as it increased wakefulness for 4 h. ABT-239 also produced such effects for 3–4 h, but it produced

a strong decrease in the theta (θ) rhythm, suggesting that the awakening effects of the drug may have been contaminated by behavioural suppressant effects.

In conclusion, lead optimization, guided mainly by calculated logP, led to the identification of an optimal compound **5a**(***SS***) (SAR110068). The compound was extensively profiled and its cardiovascular and neuropsychological/behavioural safety were assessed. SAR110068 exhibited a significant wakefulness promoting effect in EEG studies, supporting its potential therapeutic utility in human sleep–wake disorders.

Acknowledgments

The authors greatly appreciate Sanofi R&D management for the strong support, H_3R project team members for their contributions, the Sanofi analytical department for their support on analytical studies in confirmation of the structures and solid state characterizations, formulation support, and the Sanofi DMPK and Toxicology Department for PK and in vitro/in vivo safety assessments.

References and notes

1. Arrang, J. M.; Garbarg, M.; Schwartz, J. C. *Nature* **1983**, *302*, 832.
2. Chen, P. Y.; Tsai, C. T.; Ou, C. Y.; Hsu, W. T.; Jhuo, M. D.; Wu, C. H.; Shih, T. C.; Cheng, T. H.; Chung, J. G. *Mol. Med. Rep.* **2012**, *5*, 1043.
3. Bitner, R. S.; Markosyan, S.; Nikkel, A. L.; Brioni, J. D. *Neuropharmacology* **2011**, *60*, 460.
4. Ligneau, X.; Perrin, D.; Landais, L.; Camelin, J. C.; Calmels, T. P.; Berrebi-Bertrand, I.; Lecomte, J. M.; Parmentier, R.; Anaclet, C.; Lin, J. S.; Bertaina-Anglade, V.; la Rochelle, C. D.; d'Aniello, F.; Rouleau, A.; Gbahou, F.; Arrang, J. M.; Ganellin, C. R.; Stark, H.; Schunack, W.; Schwartz, J. C. *J. Pharmacol. Exp. Ther.* **2007**, *320*, 365.
5. Parmentier, R.; Anaclet, C.; Guhennec, C.; Brousseau, E.; Bricout, D.; Giboulot, T.; Bozyczko-Coyne, D.; Spiegel, K.; Ohtsu, H.; Williams, M.; Lin, J. S. *Biochem. Pharmacol.* **2007**, *73*, 1157.
6. Burban, A.; Sadakhom, C.; Dumoulin, D.; Rose, C.; Le Pen, G.; Frances, H.; Arrang, J. M. *Psychopharmacology (Berl)* **2010**, *210*, 591.
7. Inocente, C.; Arnulf, I.; Bastuji, H.; Thibault-Stoll, A.; Raoux, A.; Reimao, R.; Lin, J. S.; Franco, P. *Clin. Neuropharmacol.* **2012**, *35*, 55.
8. Medhurst, S. J.; Collins, S. D.; Billinton, A.; Bingham, S.; Dalziel, R. G.; Brass, A.; Roberts, J. C.; Medhurst, A. D.; Chessell, I. P. *Pain* **2008**, *138*, 61.
9. Yoshimoto, R.; Miyamoto, Y.; Shimamura, K.; Ishihara, A.; Takahashi, K.; Kotani, H.; Chen, A. S.; Chen, H. Y.; Macneil, D. J.; Kanatani, A.; Tokita, S. *Proc. Natl. Acad. Sci. U.S.A.* **2006**, *103*, 13866.
10. Sander, K.; Kottke, T.; Stark, H. *Biol. Pharm. Bull.* **2008**, *31*, 2163.
11. Gemkow, M. J.; Davenport, A. J.; Harich, S.; Ellenbroek, B. A.; Cesura, A.; Hallett, D. *Drug Discovery Today* **2009**, *14*, 509.
12. Gao, Z.; Hurst, W. J.; Guillot, E.; Czechtizky, W.; Lukasczyk, U.; Nagorny, R.; Pruniaux, M. P.; Schwink, L.; Sanchez, J. A.; Stengelin, S.; Tang, L.; Winkler, I.; Hendrix, J. A.; George, P. G. *Bioorg. Med. Chem. Lett.* **2013**, *23*, 3421.
13. Gao, Z.; Hurst, W. J.; Guillot, E.; Czechtizky, W.; Lukasczyk, U.; Nagorny, R.; Pruniaux, M. P.; Schwink, L.; Sanchez, J. A.; Stengelin, S.; Tang, L.; Winkler, I.; Hendrix, J. A.; George, P. G. *Bioorg. Med. Chem. Lett.* **2013**, *23*, 3416.
14. Rodriguez Sarmiento, R. M.; Nettekoven, M. H.; Taylor, S.; Plancher, J. M.; Richter, H.; Roche, O. *Bioorg. Med. Chem. Lett.* **2009**, *19*, 4495.
15. Wager, T. T.; Pettersen, B. A.; Schmidt, A. W.; Spracklin, D. K.; Mente, S.; Butler, T. W.; Howard, H.; Lettiere, D. J.; Rubitski, D. M.; Wong, D. F.; Nedza, F. M.; Nelson, F. R.; Rollema, H.; Raggon, J. W.; Aubrecht, J.; Freeman, J. K.; Marcek, J. M.; Cianfrogna, J.; Cook, K. W.; James, L. C.; Chatman, L. A.; Iredale, P. A.; Banker, M. J.; Homiski, M. L.; Munzner, J. B.; Chandrasekaran, R. Y. *J. Med. Chem.* **2011**, *54*, 7602.
16. Levoin, N.; Labeeuw, O.; Calmels, T.; Poupardin-Olivier, O.; Berrebi-Bertrand, I.; Lecomte, J. M.; Schwartz, J. C.; Capet, M. *Bioorg. Med. Chem. Lett.* **2011**, *21*, 5378. The results of Levoin's QSAR model 2 was interesting when applied to compound **1** (hERG active) and **5a**(***SS***) (hERG inactive). It was supposed that in model 2, Apol is <15473.8 (with the approximation given by the author in footnote). If AlogP was in the similar range than *c*logP, with values of 4.4 for compound **1** and 2.1 for compound **5a**(***SS***), then, hERG could be predicted as active for **1** and inactive for **5a**(***SS***).
17. Ploemen, J. P.; Kelder, J.; Hafmans, T.; van de Sandt, H.; van Burgsteden, J. A.; Saleminki, P. J.; van Esch, E. *Exp. Toxicol. Pathol.* **2004**, *55*, 347.
18. Pelletier, D. J.; Gehlhaar, D.; Tilloy-Ellul, A.; Johnson, T. O.; Greene, N. *J. Chem. Inf. Model* **2007**, *47*, 1196.
19. Gao, Z.; Hurst, W. J.; Guillot, E.; Nagorny, R.; Pruniaux, M. P.; Hendrix, J. A.; George, P. G. *Bioorg. Med. Chem. Lett.* **2013**, *23*, 4044.
20. *Analytical data for* ***5a***(***SS***): Calcd for $C_{22}H_{33}N_3O_2$: C 71.12% H 8.95% N 11.31% O 8.61%. Found: C 71.06% H 9.21% N 11.36%;
LCMS: LC method: SYNERGI 2U HYDRO-RP 20 × 4.0 mm column, 0.1% TFA in water/acetonitrile 5–40% acetonitrile in 2 min. then, to 95% acetonitrile at 5 min at flow rate of 1.0 mL/min; LCMS: R_T = 1.46 min, MS: 372 ($M+H^+$).
^1H NMR ($CDCl_3$, 300 MHz), δ (ppm): 7.34 (d, 8.2 Hz, 1H), 6.79 (s, 1H), 6.39 (s, 1H), 6.36 (s, 1H), 4.06 (m, 2H), 3.51–3.19 (m, 7H), 3.00 (m, 1H), 2.78 (m, 1H), 2.53 (m, 2H), 2.19 (s, 3H), 2.13–1.73 (m, 10H), 1.47 (m, 1H), 1.14 (d, 6.0 Hz, 3H).
21. Dressler, H.; Economides, K.; Favara, S.; Wu, N. N.; Pang, Z.; Polites, H. G. *J. Biomol. Screen* **2013**. http://dx.doi.org/10.1177/1087057113496465jbx.sagepub.com.
22. Proprietary internal in-silico model prediction. The model is based on carefully filtered internal experimental data. It was developed using relevant two- and three dimensional descriptors to capture molecular properties like shape, lipophilicity and electrostatic potential combined with powerful statistical methods. The model was carefully validated using test sets of novel molecules.
23. Griebel, G.; Decobert, M.; Jacquet, A.; Beeske, S. *Behav. Brain Res.* **2012**, *232*, 416.